F

CONF-9610210--23

SLAC-PUB-7387
October 1996

Recent Results & Plans For The Future On SLAC Damped Detuned Structures (DDS)[1]

N.M. Kroll[†‡], R.M. Jones[†‡], C. Adolphsen[†], K.L.F. Bane[†],
W.R. Fowkes[†], K. Ko[†], R.H. Miller[†],
R.D. Ruth[†], M. Seidel[†], and J.W. Wang[†]

†*Stanford Linear Accelerator Center,*
Stanford University, Stanford, CA 94309
‡ *University of California, San Diego,*
La Jolla, CA 92093-0319

Abstract

The cells in the SLAC DDS are designed in such a way that the transverse modes excited by the beam are detuned in a Gaussian fashion so that destructive interference causes the wake function to decrease rapidly and smoothly. Moderate damping provided by four waveguide manifolds running along the outer wall of the accelerator is utilised to suppress the reappearance of the wake function at long ranges where the interference becomes constructive again. The newly developed spectral function method, involving a continuum of frequencies, is applied to analyze the wake function of the DDS 1 design and to study the dependence of the wake function on manifold termination. The wake function obtained with the actually realized manifold terminations is presented and compared to wake function measurements recently carried out at the ASSET facility installed in the SLAC LINAC.

Paper presented at the 7th Workshop on Advanced Accelerator Concepts,
Lake Tahoe, CA, October 13th-19th 1996

[1] Supported by Department of Energy grant number DE-FG03-93ER40759[‡] and DE-AC03-76SF00515[†]

DISCLAIMER

Recent Results & Plans For The Future On SLAC Damped Detuned Structures (DDS)

N.M. Kroll[†‡], R.M. Jones[†‡], C. Adolphsen[†], K.L.F. Bane[†],
W.R. Fowkes[†], K. Ko[†], R.H. Miller[†],
R.D. Ruth[†], M. Seidel[†], and J.W. Wang[†]

†*Stanford Linear Accelerator Center,*
Stanford University, Stanford, CA 94309
‡ *University of California, San Diego,*
La Jolla, CA 92093-0319

Abstract. The cells in the SLAC DDS are designed in such a way that the transverse modes excited by the beam are detuned in a Gaussian fashion so that destructive interference causes the wake function to decrease rapidly and smoothly. Moderate damping provided by four waveguide manifolds running along the outer wall of the accelerator is utilised to suppress the reappearance of the wake function at long ranges where the interference becomes constructive again. The newly developed spectral function method, involving a continuum of frequencies, is applied to analyze the wake function of the DDS 1 design and to study the dependence of the wake function on manifold termination. The wake function obtained with the actually realized manifold terminations is presented and compared to wake function measurements recently carried out at the ASSET facility installed in the SLAC LINAC.

1. INTRODUCTION

The wake behind an accelerated bunch in the next linear collider (NLC) design, in which multiple bunches are accelerated within each RF pulse cycle in order to maximize the collider luminosity, has the deleterious effect of beam loading via the longitudinal wake field and a beam break up instability (1) due to the transverse wake field. It is the purpose of this work to investigate minimization of the transverse kick presented to successive bunches in the bunch train. The beam emittance is directly proportional to the mean square of the sum wake function (2) and hence in order to maintain a small beam emittance it is critical to ensure that both the short-range wake field and the long-range wake field are kept within tolerable limits. Here we are concerned with wake fields generated by previous bunches rather than intra-bunch effects, so that short-range and long-range refer to nearby and distant bunches respectively. (Present beam simulations require the

wake function be no larger than 1 V/pC/mm/m (3)). In order to reduce the amplitude of the beam-induced wake the cell frequencies are detuned in a Gaussian fashion so that the components of the resulting wake field interfere destructively, causing the wake function to decrease rapidly and smoothly. However, eventually the interference becomes at least in part again constructive leading to reappearance of the wake at an unacceptable amplitude, and one either adopts a method of interleaving a set of multiple structures, each with a slightly different central frequency (to delay reappearance to distance beyond the end of the bunch train) or one utilizes moderate damping to suppress reappearance; the former method entails very tight structure tolerances whereas the latter involves an order of magnitude looser tolerances. The manifold damping scheme provides two additional advantages: significantly enhanced beam diagnostic capability and improved pumping capability for the accelerator structure.

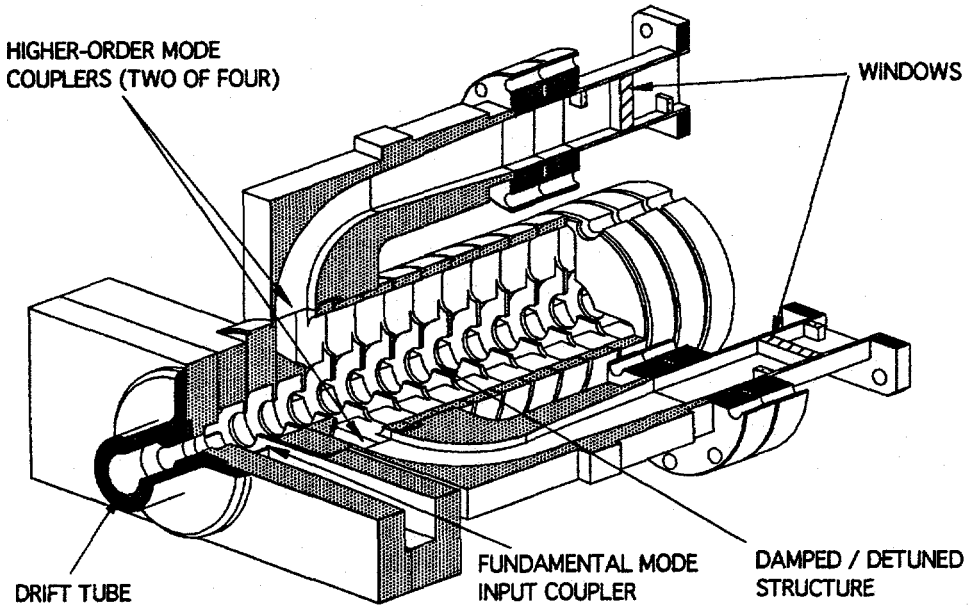

FIGURE 1. Cut-Away View of DDS.

A cross-sectional view of the DDS is shown in fig.1. The features which prove crucial to the reduction of the wake field are clearly illustrated: viz., the tapered cells in cross section and the tapered manifolds, of which two of the four are shown, running parallel to the axis of the accelerator. The figure also shows the way in which the manifolds are coupled to matched loads. The manifold is connected to a rectangular waveguide by means of a 90 degree mitered bend followed by a 90 degree circular H-bend, a taper to WR62 waveguide, a rectangular window, and finally (not shown) a matched load. As will be discussed later the quality of the match to the manifold achieved by this assembly

has a very significant effect on the long range wake. Here the concept of "match" applies only to frequencies at which the manifold is propagating. Frequencies for which the manifold is non-propagating at *both* ends will be referred to as stop bands, other frequencies as pass bands.

In the following we report on the computational methods employed, the application of the spectral function method to DDS 1, and our investigation of the sensitivity of the wake function to manifold mismatch. The final section incorporates a new design which results in a considerably reduced short range wake and with prospects for further improvements to the long-range wake function.

2. METHOD OF WAKE FUNCTION CALCULATION

All of our wake function calculations are based upon the equivalent circuit network given in (4), consisting of a sequence of sections each one of which corresponds to a cell and the contiguous section of manifold. The full description of the structure includes a set of 10 "model" parameters for each section. The frequency domain circuit equations are cast in matrix form as (schematically) follows:

$$\begin{pmatrix} \hat{H} & H_x^t \\ H_x & H - GR^{-1}G \end{pmatrix} \begin{pmatrix} \hat{a} \\ a \end{pmatrix} - f^{-2} \begin{pmatrix} \hat{a} \\ a \end{pmatrix} = f^{-2} \begin{pmatrix} B \\ 0 \end{pmatrix} \tag{2.1}$$

Here each component of the column matrices is an N component vector, and the elements of the square matrix are N by N matrices. The number of sections, N, is taken to be 206 for all calculations reported here. The column matrix on the LHS of (2.1) represents the cell excitation, that on the RHS the drive beam, and f is the frequency. The effect of the manifold is contained in the damping matrix $GR^{-1}G$. There are three possible regimes in which the transverse wake function (i.e. wake potential per unit length) for a particle trailing a distance s behind a velocity c drive bunch (per unit drive bunch charge per unit drive bunch displacement) may be calculated, viz., no damping, weak damping and strong damping:

$$W(s) = 2\sum_{i=1}^{P} K_p \sin\left(\frac{2\pi f_p}{c} s\right) \theta(s) \tag{2.2}$$

$$W(s) = 2\sum_{i=1}^{P} K_p \sin\left(\frac{2\pi f_p}{c} s\right) \exp\left(-\frac{2\pi f_p}{Q_p c} s\right) \theta(s) \tag{2.3}$$

$$W(s) = \int_{f>0} S(f) \sin\left(\frac{2\pi f}{c} s\right) df \, \theta(s) \tag{2.4}$$

Here $\theta(s)$ is the unit step function and, K_p, f_p, and Q_p the p-th modal kick factor (5), frequency, and quality factor, respectively. The wake for the first two cases (eqns. 2.2 & 2.3) are expressed as modal sums, while the third (eqn 2.4) encompasses a continuum of modes and is the regime of the spectral function (6). The spectral function S(f) consists of a sum of terms of the form $2\,K_p\,\delta(f-f_p)$ for f in a stop band and a continuous function defined below for f in a pass band. The form (2.4) encompasses the other two as limiting cases.

2.1 Modal Sums and the Perturbation Method

We can obtain the K_p and f_p of (2.2) by setting the RHS and the damping matrix of (2.1) equal to zero, and finding the mode frequencies (real, of course in this case) and amplitude vectors (also real) for which the resultant equation for the amplitudes has non trivial solutions. The K_p are formed from the mode vectors as described in (5), and the undamped wake function (2.2) formed. These results provide the basis for the perturbation method described below. It has turned out to be useful to construct a smoothed spectral function, $S_s(f)$ to represent these results:

$$S_s(f) = 2K_p / (f_{p+1} - f_p), \quad f_p < f < f_{p+1}, \ \forall p \tag{2.5}$$

The dashed curve of Fig. 6 is an example.

For sufficiently weak damping one can obtain the form eqn. (2.3) by making use of the perturbation formula (7)

$$\delta f_p / f_{p_0} = \tfrac{1}{2} f_{p_0}^2 a_{p_0}^\dagger G R^{-1} G a_{p_0} / (a_{p_0}^\dagger a_{p_0}) \tag{2.6}$$

which is valid to an excellent approximation for small frequency shifts (7).

Here f_{p_0} is the unperturbed p'th modal frequency, G describes the coupling to the manifold, and a_{p_0} is the p'th unperturbed eigenmode. The Q from this equation, together with values obtained from an exact calculation of the complex eigenmodes are shown in figs. 2. The detuning behaves in a similar manner. These results indicate that perturbation theory is unreliable for the DDS 1 parameters. The fact that the absolute value of the perturbation theory complex frequency shift is significantly larger than the mode separation at the center of the band is a strong warning that this will be the case.

The exact eigenmodes and eigenfrequencies can be used to construct a damped modal sum representation of the wake function similar in form to the above (4)(8), and in good agreement with the results obtained by the

spectral function method discussed below. The latter is preferred because it is theoretically better founded and far simpler computationally. Indeed

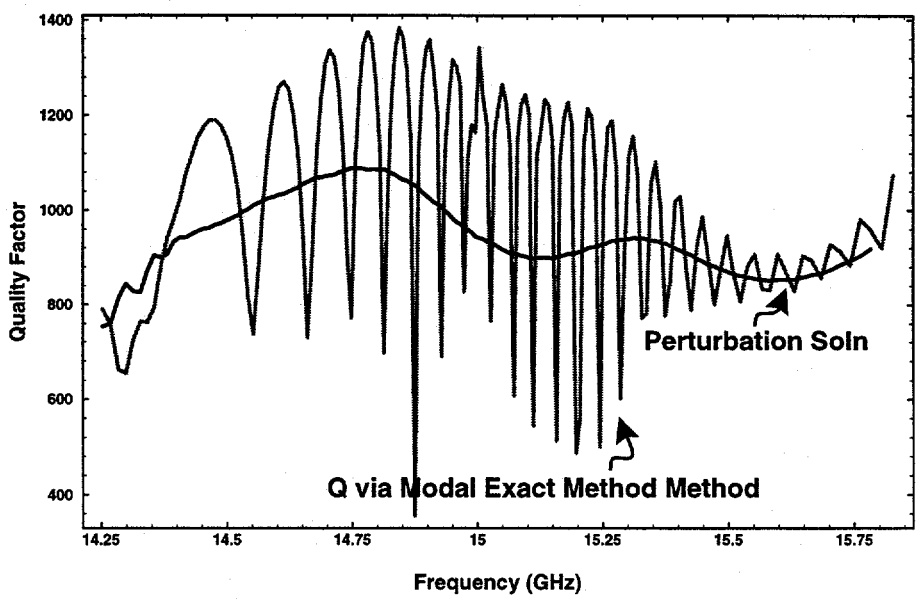

FIGURE 2. Manifold loaded Q. The Q of the DDS is highly oscillatory ranging from 400 to 1400, characteristic of an overcoupled system. The oscillations are centered about the values obtained from petrurbation theory

the numerical difficulties encountered in determining exact eigenmodes and frequencies indicated that it is not a practical method for extensive investigation.

2.2 The Spectral Function Method

In a somewhat more condensed notation eqn. (2.1) may be written:

$$\overline{\overline{H}}\,\overline{a} - f^{-2}\overline{a} = f^{-2}\overline{B} \tag{2.7}$$

Where the 2N component column vector on the right hand side of eqn. (2.7) represents the drive beam. The wake function is evaluated in terms of the drive beam B, and after some considerable algebraic and matrix manipulations it is evaluated in the form (2.4) where the spectral function is given by:

$$S(f) = 4\pi^{-1}\,\mathrm{Im}\left\{\sum_{n,m}^{N}\sqrt{K_s^n K_s^m f_s^n f_s^m}\,\exp[(2\pi jL/c)(f+j\varepsilon)(n-m)]\tilde{H}_{nm}\right\} \tag{2.8}$$

Here L is the cell period, f_s^n and K_s^n, are the synchronous frequency and kick factor respectively, and ε is an infinitesimal quantity (6). The envelope of the

wake function is given in terms of the absolute value of the Fourier transform of S(f):

$$W_c(s) = \theta(s)\left|\int_0^\infty S(f)\exp[(2\pi j s/c)f]\,df\right| \tag{2.9}$$

In applying this technique S(f) in eqn. (2.8) is sampled in the pass band region for, 2000 or so frequencies and the FFT (Fast Fourier Transform) is evaluated. A typical example of a spectral function in a well damped case is seen in Fig. 6. The individual damped modes appear as oscillations about the smoothed S(f) with the more weakly damped modes being more prominent. The beat-like character of the oscillation echoes the Q oscillations seen in Fig. 2.

3. APPLICATION OF THE THEORY TO DDS 1 AND COMPARISON WITH EXPERIMENT.

The first applications of the spectral function method have been to the DDS 1 structure. The spectral function and wake envelope function for the matched manifold case are given in (6) and (9) The method has been used to study the effect of manifold mismatch on the wake-function. An example is provided by Figs. 3 and 4. Fig. 4 shows that wake quality is much more sensitive to downstream mismatch than to upstream mismatch, and Fig. 3 shows correspondingly that spectral function smoothness is much more degraded for the downstream case.

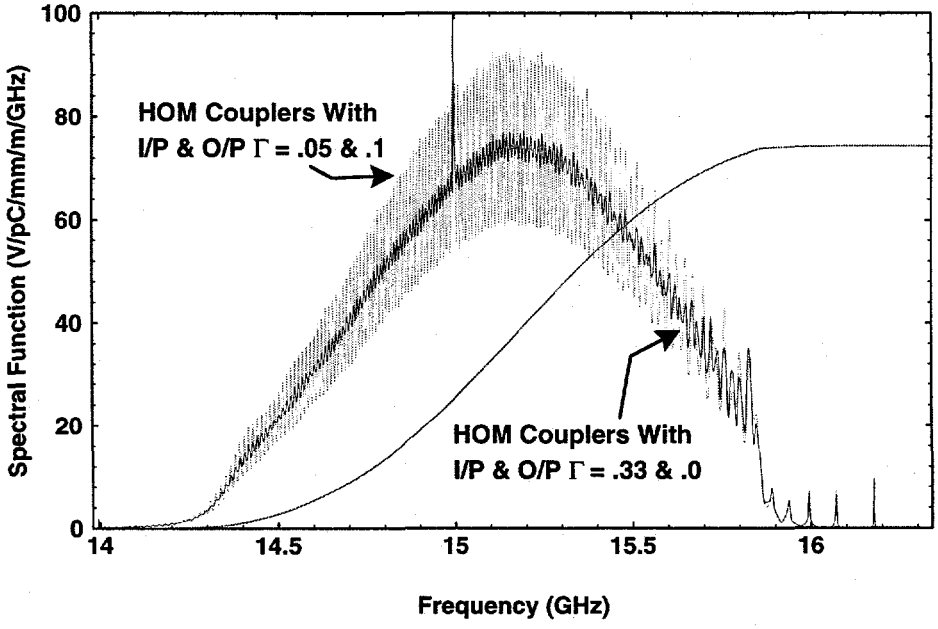

FIGURE 3. Two spectral functions, one incorporating a large mismatch in the input HOM coupler and another including a modest mismatch in the output HOM coupler.

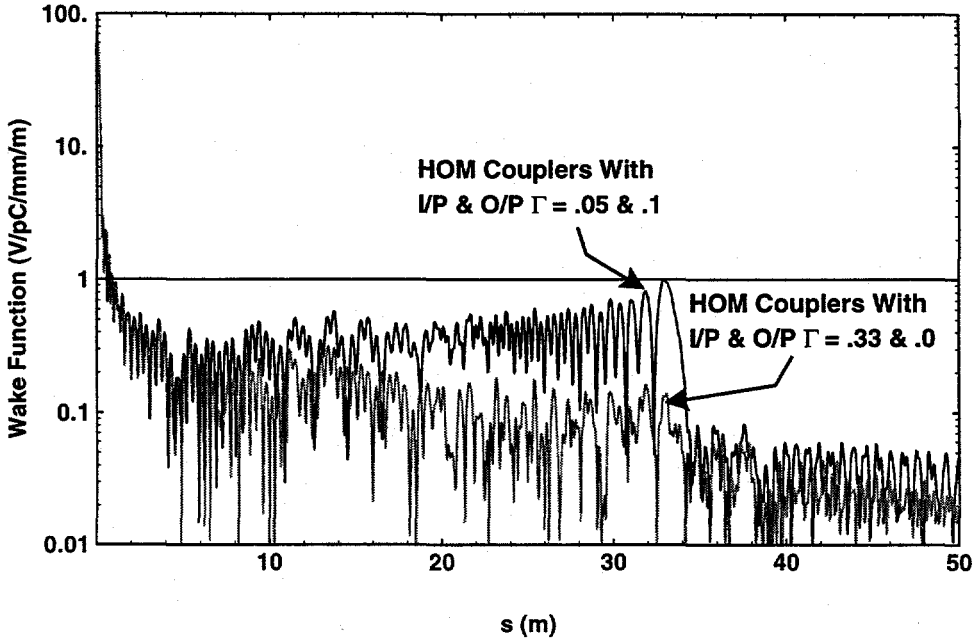

FIGURE 4. Wake function calculated via the spectrum method in which the directional sensitivity of the wake on the input and output HOM couplers is illustrated. The relatively modest mismatch in the output HOM coupler has a significant adverse affect on the wake function (whereas the wake function is relatively insensitive to substantial mismatches in the input HOM coupler)

The manifold terminations actually used in DDS 1 are discussed in (10). The mismatch is substantial and has two principal sources, namely the mitered bend and the rectangular windows (Fig. 1). The downstream manifold is close to cutoff at the low frequency end of the relevant spectral region and is poorly matched there. The windows, which were the only ones available, are poorly matched at the high frequency end.

The resultant spectral function is shown in (6), and the wake envelope function is shown in Fig. 5.

The wake for DDS 1 was measured experimentally in the SLAC LINAC ASSET facility and the results reported in (9). The experimental points shown on the curve in Fig. 5 were obtained from these measurements. The agreement is considered to be reasonably satisfactory given various differences (some planned, some inadvertent) between the DDS model and DDS 1 as fabricated.

4. REDESIGNED DAMPED DETUNED STRUCTURES

In our design of DDS 1 we chose eleven representative sections to obtain frequency-phase pairs from detailed MAFIA simulations and hence obtain

ten model parameters (nine circuit parameters plus the cell kick-factors) for each of the eleven sections. Parameters for all sections are subsequently obtained by error function fits and interpolation. A similar procedure may be followed to

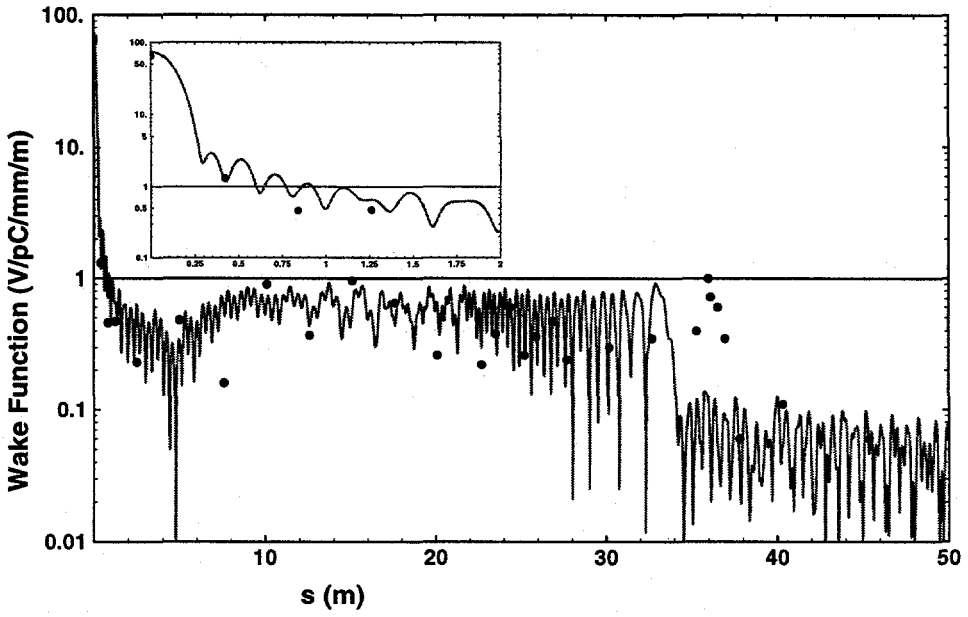

FIGURE 5. Wake function calculated via the spectrum method in which the effect of mismatches in the mitered bend and windows of the higher order mode couplers (HOM) are included. Data determined from the ASSET experiment on the SLC are indicated with dots. The short range wake function is shown inset.

determine the five geometric parameters (i.e., dimensions) (8) for all the sections from those for the original eleven. This is a substantial task for each structure design. However, as we now have all fifteen parameters as a function of synchronous frequency, we can take advantage of this functional dependence to explore new design distributions and to obtain the set of section dimensions which would be needed to realize them. Our new design incorporates a Gaussian kick factor weighted density function with a bandwidth of 5 units of sigma, or 11.25% in units of the central dipole frequency, and the sigma of the Gaussian is 2.25% of the central frequency. Based on our fit parameters we prescribe a smooth uncoupled spectral function, $S_0(f_s)\lambda$ and impose the condition that: $2K(f_s)dn/df = S_0(f_s)\lambda$, where λ is a scale factor to be determined. The upper and lower truncation bounds on the synchronous frequencies are imposed, f_{s1} and f_{sN} and the normalisation condition is obtained:

$$\lambda = N / \int_{f_{s1}}^{f_{sN}} (\tfrac{1}{2} S_0 / K) df_s \qquad (4.1)$$

Then the new synchronous frequencies are determined according to:

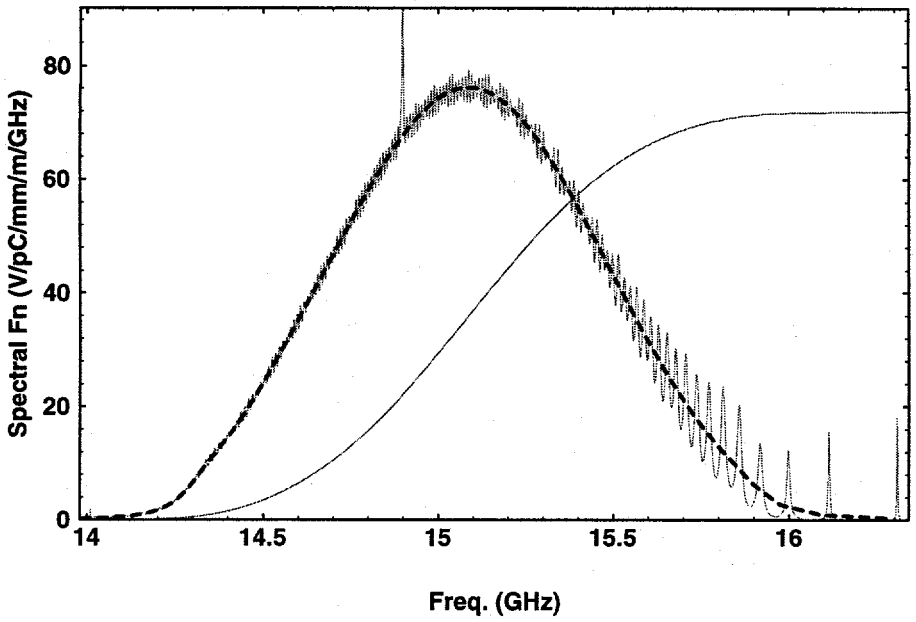

FIGURE 6. Spectral function for proposed DDS with a bandwidth of 5 units of σ width (a frequency bandwidth of 11.25% of the central frequency, and σ is 2.25% of the central frequency). This DDS incorporates perfectly matched HOM couplers terminated in perfectly matched loads. Also shown, dashed and, running through the center of the oscillating spectral function, is the spectral function corresponding to the idealized case (G = 0). The latter spectral function provides a goal in future design strategies.

$$\int_{f_{sn}}^{f_{sn+1}} \frac{1}{2K} \lambda S_0 df_s = 1 \tag{4.2}$$

This enables all the cell synchronous frequencies to be determined and hence the new ten parameters are determined. The smoothed spectral function (shown dashed in Fig. 6) is seen to possess the smooth Gaussian form which was the aim of the design procedure.

The spectral function itself (the oscillatory curve in Fig. 6) exhibits the underlying damped mode structure as mentioned previously. The more pronounced oscillations in the upper part of the frequency interval (approximately 15.5 GHz and thereafter) can be reduced by including an enhanced tapered coupling for the last 20 or so cells (11). These more prominent oscillations are responsible for the slight increase of the wake envelope function in the 5 meter region (Fig. 7). The new design has, however, a significantly improved short range wake field, in particular for the first bunch, which sees a wake field an order of magnitude weaker than that seen in DDS 1. An ideally damped design would lead to a spectral function which coincides with the smoothed S(f); the resultant idealized wake envelope function is also shown in Fig. 7.

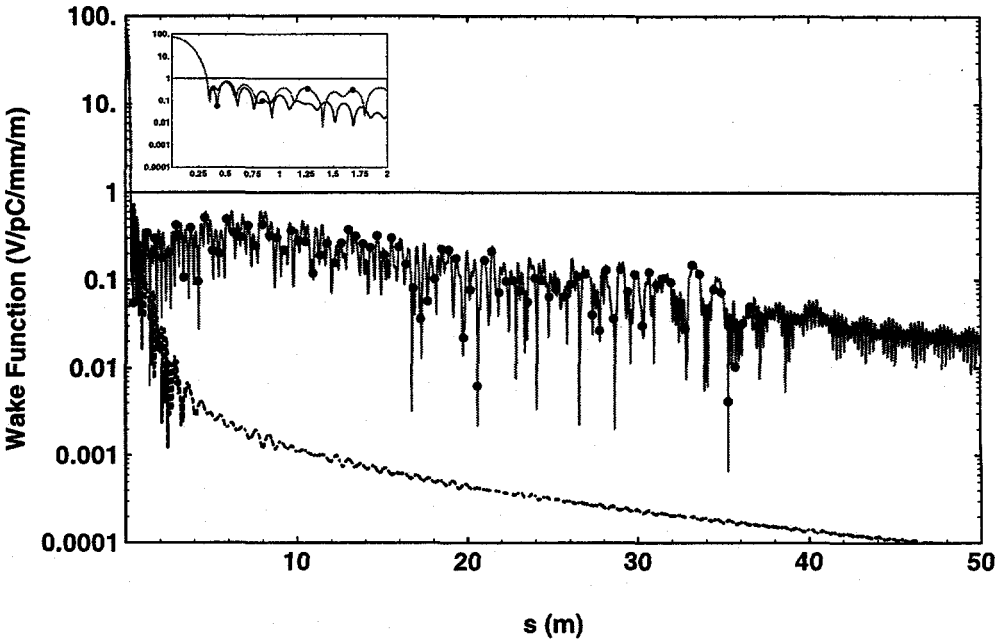

FIGURE 7. Wake envelope function generated by the spectral function of Fig. 6. The dots indicate the positioning of bunches spaced at 1.4ns intervals (not experimental points). The lower curve is the idealized wake function generated by the dashed curve of Fig. 6.

5. ACKNOWLEDGEMENTS

This work is supported by Department of Energy grant number DE-FG03-93ER40759[‡] and DE-AC03-76SF00515[†]. We have benefited greatly from discussions at the weekly structures meeting at SLAC, where these results were first presented and thank all members of the group.

6. REFERENCES

1. Neal, R.B and Panofsky, W.H., *Science*, **152,** 1353 (1966)
2. Bane, K.L.F et al, EPAC94, London, England, 1994; SLAC-PUB- 6581
3. Thompson, K.A., private communication, 1996.
4. Jones, R.M., Ko, K., Kroll, N.M. , Miller, R.H., & Thompson, K.A, EPAC96, Sitges, Spain, June 10-14, 1996; SLAC-PUB-7187 (http://libnext.slac.stanford.edu/slacpubs/7000/slac-pub-7187.ps.Z)
5. Bane, K.L.F, and Gluckstern, R., *Part. Accel.*, **42,** 123 (1993); SLAC-PUB-5783
6. Jones, R.M., Ko, K., Kroll, N.M., & Miller, R.H., Linac96; SLAC-PUB-7287
7. Jones, R.M., Kroll, N.M. & Miller R.H., To be submitted to *Phys. Rev. E*, 1997
8. Ko, K. et al, PAC95, Dallas, Texas; SLAC-PUB-95-6844
9. Miller, R.H. et al, Linac96, Geneva, Switzerland, 1996; SLAC-PUB -7288
10. Seidel, M., et al, Linac96, Geneva, Switzerland,, 1996; SLAC-PUB-7289
11. Jones, R.M., Kroll, N.M. & Miller, R.H., to be submitted to PAC 97